



Sailboat Path Following Control Based on LOS with Sideslip Angle Observation and Finite-Time Backstepping

Kangjian Shao¹, Yujin Wu¹, Ning Wang²(✉), and Hongde Qin¹

¹ Harbin Engineering University, Harbin 150001, China

² Dalian Maritime University, Dalian 116026, China

n.wang@ieee.org

Abstract. Suffering from complex sideslip angles, path following control of sailboat becomes significantly challenging. In this article, double finite-time observers-based line-of-sight guidance and finite-time control (DFLOS-FC) scheme is presented for path following of sailboat. Double finite-time sideslip observers (DFSO) are employed to observe the time-varying sideslip angle caused by external disturbances, which improves the accuracy of line-of-sight guidance. To avoid differential explosion problem caused by virtual control law, we designed a finite-time filter. The finite-time disturbance observer (FDO) is designed to accurately observe unknown external disturbances, which enables the controller to have excellent tracking accuracy and precise disturbance rejection. Considering the rotation limit of actuator rudder angle, we limit the rudder angle. The finite-time stability of the integrated guidance and control system is strictly guaranteed by Lyapunov method. Finally, the effectiveness of this method is verified by simulation and comparison with the traditional backstepping method.

Keywords: Sideslip Angle Observation · Line-of-sight Guidance · Finite-time Control · Sailboat · Path following

1 Introduction

As underactuated marine vehicles (USV) play an outstanding role in port protection, mine countermeasures, reconnaissance and surveillance tasks [1], they have attracted wide attention in recent years. When performing a mission, most of the USV's energy is used for propulsion, which reduces the USV's endurance, while the sailboat relies on wind, which reduces energy consumption and is suitable for large-scale and long-term missions. Therefore, the study of unmanned sailboat is of great significance for marine exploration and environmental monitoring.

Autonomous navigation is the core technology of unmanned sailboats, and how to make good decisions and control is a problem to realize autonomous navigation. In [2], Wang proposed an autonomous navigation scheme for the first time for USV that integrates waypoint generation, path smoothing and policy guidance, which perfectly

combined decision-making and control. In terms of control, path following is the key technology to achieve autonomous navigation, so it is necessary to study path following control of sailboat. The path following of the sailboat includes guidance and control goals. Guidance is the specific method to guide the sailboat to reach a certain point or reference route; control refers to the execution strategy of implementing the guidance.

The technology of line-of-sight (LOS) guidance is widely used in USV. In [3], LOS was applied to the way-point tracking control. In [4], Li designed integral LOS (ILOS) for underactuated vessels, which successfully implemented point-to-point navigation. In actual navigation, the sideslip angle is complex and time-varying, which affects the accuracy of LOS guidance. In [5], Wan designed a reduced-order state observer, which can estimate the time-varying sideslip angle online, thus improving the accuracy of LOS guidance. In [6], Su proposed an improved adaptive integral LOS (AILOS), which constructed three adaptive variables to replace the unmeasurable current and sideslip angle, and adjusted the adaptive variables online according to the tracking error, thus reducing the error. In [7], the complex sideslip angle is estimated by an improved extended state observer based LOS (ELOS). The precise observation of sideslip angle is of great significance to the path tracking of sailboat, but there are still few related studies.

Due to the uncertainty and complexity of the actual ocean environment, it is difficult to establish an accurate mathematical model for sailboat [8]. For computational convenience, the model is usually simplified. In previous studies, most scholars ignored the rolling motion [9–11], but the sailboat needs to consider the roll response due to the existence of the sail. In [12], Xiao proposed the four-degree-of-freedom mathematical model of keel-sailboat, took roll moment into consideration. However, external disturbances are not considered in [12]. To ensure the accuracy of the simulation, the uncertainty of external disturbances need to be considered [13, 14]. In [15], finite-time differentiator (FTD) was designed for disturbance estimation, and good observation results have been achieved. In [16], Wang designed a single-hidden layer feedforward network based adaptive compensating identifier (SACI), which can compensate for the overall uncertainty. Neural networks and fuzzy logic systems are also commonly used to approximate unknown models and external disturbances [17–20], but neural networks will increase the amount of computation, and fuzzy logic systems are difficult to build. In [21], Rong devised an adaptive nonlinear disturbance observer (NDO) to observe the uncertainty of external disturbances and model, and obtained the accurate observation results. Path following is a key technology in the field of control. Nowadays, the technology about path following is becoming more and more mature. In [22], a coordinated trajectory-tracking control (CTTC) scheme was designed for path following of marine aerial-surface heterogeneous (MASH) system, and high tracking accuracy was obtained. In [16], Wang proposed a finite-time unknown observer-based interactive trajectory tracking control (FUO-ITTC) scheme, which has remarkable performance in terms of transient and steady-state tracking accuracy. In [23], accurate trajectory tracking problem of a surface vehicle disturbed by complex marine environments is solved by creating a finite-time control (FTC) scheme, and both disturbance observation and trajectory tracking errors can exactly reach to zero in a finite time. But finite-time stability of heading control system is also not taken into account by the existing methods.

Driven by the above observations, the double finite-time observers-based LOS guidance and finite-time control (DFLOS-FC) scheme is proposed, and the contributions of this article are summarized as follows:

- (1) The DFSO devised in this paper can observe time-varying sideslip angle, which can be applied to more complex working conditions.
- (2) In order to prevent the large amount of computation caused by the direct derivation of the virtual control law, a finite-time filter is introduced in this paper.
- (3) The finite-time disturbance observer (FDO) is introduced to compensate for external disturbances, so that the controller has high control accuracy.

This paper is arranged as follows: In Sect. 2, the problem formulation and some preliminaries are put forward. We design double finite-time sideslip angle observers for sideslip observation in Sect. 3. Section 4 presents the design and stability analysis of the sailboat controller. In Sect. 5, the simulation is carried out. Conclusions are drawn in Sect. 6.

2 Preliminaries and Problem Formulations

2.1 Preliminaries

Lemma 1: ([23]) For system

$$\dot{x} = f(x) \quad (1)$$

Suppose there exist a continuously differentiable function $V(x)$, which satisfies

$$\dot{V}(x) \leq -aV(x) - bV^\rho(x) + c \quad (2)$$

where $a > 0, b > 0, 0 < \rho < 1, 0 < c < \infty$.

Then the trajectory of system $\dot{x} = f(x)$ can achieve finite time stability. In addition, the finite setting time T_f satisfies

$$T_f = \max \left\{ t_0 + \frac{1}{a\theta_0(1-l)} \ln \frac{\theta_0 a V^{1-\rho}(t_0) + b}{b}, t_0 + \frac{1}{a(1-l)} \ln \frac{a V^{1-\rho}(t_0) + \theta_0 b}{\theta_0 b} \right\} \quad (3)$$

Lemma 2: ([24]) The following system:

$$\begin{aligned} \dot{\sigma}_0 &= -\lambda_0 L^{1/(n+1)} |\sigma_0|^{n/(n+1)} \text{sign}(\sigma_0) + \sigma_1 \\ \dot{\sigma}_1 &= -\lambda_1 L^{1/n} |\sigma_1 - \dot{\sigma}_0|^{(n-1)/n} \text{sign}(\sigma_1 - \dot{\sigma}_0) + \sigma_2 \\ &\vdots \\ \dot{\sigma}_{n-1} &= -\lambda_{n-1} L^{1/2} |\sigma_{n-1} - \dot{\sigma}_{n-2}|^{1/2} \text{sign}(\sigma_{n-1} - \dot{\sigma}_{n-2}) + \sigma_n \\ \dot{\sigma}_n &\in [-\lambda_n L \text{sign}(\sigma_{n-1} - \dot{\sigma}_{n-2}) + [-L, L]] \end{aligned} \quad (4)$$

is finite-time stable, where $L > 0, \lambda_i > 0, i = 0, 1, 2, \dots, n$.

2.2 Problem Formulations

As shown in Fig. 1, taking a 4-DOF sailboat as an example, its motion can be described by body-referenced frame and inertial-referenced frame. The 4-DOF sailboat kinematic and kinetic model can be expressed as follows [12]:

$$\begin{cases} \dot{x} = u \cos(\psi) - v \cos(\phi) \sin(\psi) \\ \dot{y} = u \sin(\psi) + v \cos(\phi) \cos(\psi) \\ \dot{\phi} = p \\ \dot{\psi} = r \cos(\phi) \end{cases} \quad (5)$$

$$\begin{cases} m_u \dot{u} = F_{Su} + F_{Ru} - F_{Ku} + m_v vr - F_{Du} + d_{wu} \\ m_v \dot{v} = F_{Sv} + F_{Rv} - F_{Kv} + m_u ur - F_{Dv} + d_{wv} \\ m_p \dot{p} = M_{Sp} + M_{Rp} - M_{Kp} - c|p|p - a\phi^2 - b\phi - M_{Dp} + d_{wp} \\ m_r \dot{r} = M_{Sr} + M_{Rr} - M_{Kr} - (X_{\dot{u}} - Y_{\dot{v}})uv - M_{Dr} - d|r|r \cos(\phi) + d_{wr} \end{cases} \quad (6)$$

where $m_u = m - X_{\dot{u}}$, $m_v = m - Y_{\dot{v}}$, $m_p = I_{xx} - K_{\dot{p}}$, $m_r = I_{zz} - N_{\dot{r}}$, and the forces and torques generated by the rudder, sail, keel and hull of the sailboat are denoted as F_{ij} and M_{ij} ($i = R, S, K, D, j = u, v, p, r$). d_{wi} ($i = u, v, p, r$) are external disturbances. (x, y) and (ϕ, ψ) represent the position and direction of the sailing boat respectively. (u, v) denotes linear velocity and (p, r) denotes angular velocity.

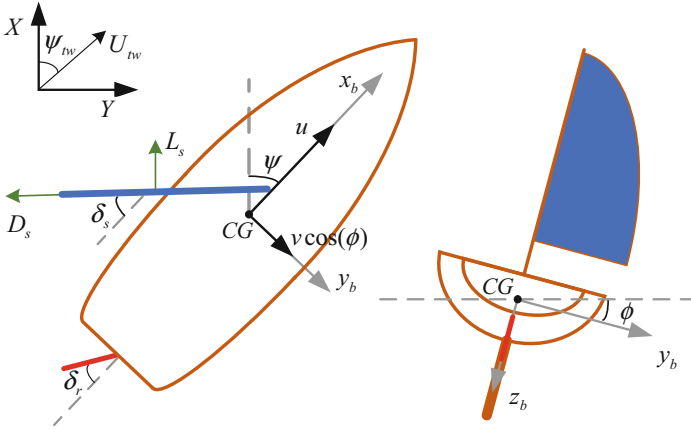


Fig. 1. Illustration of kinetic variables

The attack angle of sail is

$$\alpha_s = \alpha_{aw} - \delta_s \quad (7)$$

where α_w is apparent wind angle, δ_s is sail angle.

The lift and drag forces of the sail can be written as

$$\begin{cases} L_s = \frac{1}{2} \rho_a A_s V_{as}^2 C_{Ls}(\alpha_s) \\ D_s = \frac{1}{2} \rho_a A_s V_{as}^2 C_{Ds}(\alpha_s) \end{cases} \quad (8)$$

where ρ_a is air density, V_{as} is apparent wind speed, A_s denotes the area of the sail, the coefficients of lift and drag are denoted as $C_{Ls}(\alpha_s)$, $C_{Ds}(\alpha_s)$.

Assuming that there is no effect of current, we get $\alpha_s = -\delta_r$. The steering moment generated by the rudder can be written as

$$M_{Rr} = -\frac{1}{2} \rho_w A_r V_{ar}^2 |x_r| C_{Lr}(-\delta_r) \quad (9)$$

where ρ_w denotes seawater density, A_r denotes the area of the rudder, x_r denotes the value of the rudder's center of gravity on the x-axis in the body-referenced frame. V_{ar} denotes the apparent speed of the rudder and $C_{Lr}(-\delta_r)$ denotes the lift coefficient of the rudder. And one can get more details on the model in [12].

According to the manual sailing experience, the value range of the apparent wind angle of tacking is $0^\circ \sim \pm 30^\circ$ and the value range of the apparent wind angle of windward sailing is $\pm 30^\circ \sim \pm 160^\circ$. The sail angle is set to 0° , the sail angle is set by linear interpolation and the rotation limit of the sail angle is set as $\pm 90^\circ$. The apparent wind angle of gybing is $\pm 160^\circ \sim \pm 180^\circ$, then the sail angle is set to $\pm 90^\circ$.

3 Sideslip Angle Observation and Line-Of-Sight Guidance

In this section, double finite-time sideslip observers are designed for sideslip angle observation.

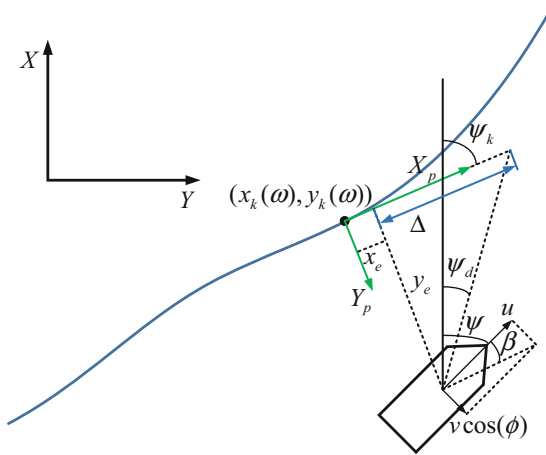


Fig. 2. Framework of LOS guidance

As shown in Fig. 2, ω is the path parameter variable, which determines the shape of the path. $(x_k(\omega), y_k(\omega))$ is a point on the prescribed path, the tangent angle of any point on the path can be denoted as $\psi_k = \arctan(\dot{y}'_k/\dot{x}'_k)$, and (x, y) is the current position of the sailboat. Then the position error can be described as

$$\begin{bmatrix} x_e \\ y_e \end{bmatrix} = \begin{bmatrix} \cos(\psi_k) & \sin(\psi_k) \\ -\sin(\psi_k) & \cos(\psi_k) \end{bmatrix} \cdot \begin{bmatrix} x - x_k(\omega) \\ y - y_k(\omega) \end{bmatrix} \quad (10)$$

The time derivative of (10) is

$$\begin{cases} \dot{x}_e = (\dot{x} - \dot{x}_k) \cos(\psi_k) + (\dot{y} - \dot{y}_k) \sin(\psi_k) + \dot{\psi}_k y_e \\ \dot{y}_e = -(\dot{x} - \dot{x}_k) \sin(\psi_k) + (\dot{y} - \dot{y}_k) \cos(\psi_k) + \dot{\psi}_k x_e \end{cases} \quad (11)$$

Substituting (9) into (11), we have:

$$\begin{cases} \dot{x}_e = U \cos(\psi - \psi_k + \beta) + \dot{\psi}_k y_e - u_p \\ \dot{y}_e = U \sin(\psi - \psi_k + \beta) - \dot{\psi}_k x_e \end{cases} \quad (12)$$

where the resultant speed of the sailboat is denoted as $U = \sqrt{u^2 + (v \cos(\phi))^2}$, $\beta = \arctan(v \cos(\phi)/u)$ is sideslip angle of sailboat, and $u_p = \dot{\omega} \sqrt{x_k'^2 + y_k'^2}$ denotes the speed of the virtual target point.

The speed u_p can be selected as

$$\begin{aligned} u_p &= U \cos(\psi - \psi_k + \hat{\beta}) + k_x x_e \\ \dot{\omega} &= \frac{U \cos(\psi - \psi_r + \hat{\beta}) + k_x x_e}{\sqrt{x_r'^2 + y_r'^2}} \end{aligned} \quad (13)$$

where k_x is a positive tuning parameter.

Double finite-time sideslip angle observer is designed as

$$\begin{cases} \dot{\hat{x}}_e = -\lambda_1 \text{sig}^{4/5}(\tilde{x}_e) + \hat{h}_1 + \dot{\psi}_k y_e - u_p \\ \dot{\hat{h}}_1 = -\lambda_2 \text{sig}^{3/5}(\tilde{x}_e) + \vartheta_1 \text{sign}(\tilde{x}_e) \end{cases} \quad (14)$$

$$\begin{cases} \dot{\hat{y}}_e = -\lambda_3 \text{sig}^{4/5}(\tilde{y}_e) + \hat{h}_2 - \dot{\psi}_k x_e \\ \dot{\hat{h}}_2 = -\lambda_4 \text{sig}^{3/5}(\tilde{y}_e) + \vartheta_2 \text{sign}(\tilde{y}_e) \end{cases} \quad (15)$$

where $h_1 = U \cos(\psi - \psi_k + \beta)$, $h_2 = U \sin(\psi - \psi_k + \beta)$, $\lambda_i (i = 1, 2, 3, 4)$ and $\vartheta_j (j = 1, 2)$ are tuning parameters, \hat{x}_e , \hat{h}_1 , \hat{y}_e and \hat{h}_2 are the estimates of x_e , h_1 , y_e and h_2 . Let $\tilde{x}_e = \hat{x}_e - x_e$, $\tilde{h}_1 = \hat{h}_1 - h_1$, $\tilde{y}_e = \hat{y}_e - y_e$, $\tilde{h}_2 = \hat{h}_2 - h_2$, the time derivative of \tilde{x}_e , \tilde{h}_1 , \tilde{y}_e , \tilde{h}_2 are

$$\begin{cases} \dot{\tilde{x}}_e = -\lambda_1 \text{sig}^{4/5}(\tilde{x}_e) + \tilde{h}_1 \\ \dot{\tilde{h}}_1 = -\lambda_2 \text{sig}^{3/5}(\tilde{x}_e) \end{cases} \quad (16)$$

$$\begin{cases} \dot{\tilde{y}}_e = -\lambda_3 \text{sig}^{4/5}(\tilde{y}_e) + \tilde{h}_2 \\ \dot{\tilde{h}}_2 = -\lambda_4 \text{sig}^{3/5}(\tilde{y}_e) \end{cases} \quad (17)$$

According to [25], there is a finite time $0 < T_\beta < \infty$ that makes $\hat{x}_e \equiv x_e$, $\hat{h}_1 \equiv h_1$, $\hat{y}_e \equiv y_e$, $\hat{h}_2 \equiv h_2$. The estimated sideslip angle is

$$\hat{\beta} = \text{arc sin} \left(\frac{\hat{h}_2 \cos(\psi - \psi_k) - \hat{h}_1 \sin(\psi - \psi_k)}{U} \right) \quad (18)$$

Then the error of sideslip angle is expressed as

$$\tilde{\beta} = \text{arc sin} \left(\frac{\tilde{h}_2 \cos(\psi - \psi_k) - \tilde{h}_1 \sin(\psi - \psi_k)}{U} \right) \quad (19)$$

Therefore, the observed error of sideslip angle converges to zero in finite time. The LOS method tracking angle is expressed as

$$\psi_d = \psi_k - \arctan \left(\frac{y_e}{\Delta} \right) - \hat{\beta} \quad (20)$$

where Δ denotes a look-ahead distance.

Substituting (13) and (20) into (12), we have

$$\begin{cases} \dot{x}_e = -k_x x_e + \dot{\psi}_k y_e \\ \dot{y}_e = -\frac{U y_e}{\sqrt{y_e^2 + \Delta^2}} \cos(\tilde{\beta} + \tilde{\psi}) - \frac{U \Delta}{\sqrt{y_e^2 + \Delta^2}} \sin(\tilde{\beta} + \tilde{\psi}) - \dot{\psi}_k x_e \end{cases} \quad (21)$$

Choose the Lyapunov function $V_1 = \frac{1}{2}x_e^2 + \frac{1}{2}y_e^2$, and the derivative of V_1 gives:

$$\begin{aligned} \dot{V}_1 &= x_e \dot{x}_e + y_e \dot{y}_e \\ &= -k_x x_e^2 + \dot{\psi}_k y_e x_e - \frac{U y_e^2}{\sqrt{y_e^2 + \Delta^2}} \cos(\tilde{\beta} + \tilde{\psi}) \\ &\quad - \frac{U \Delta y_e}{\sqrt{y_e^2 + \Delta^2}} \sin(\tilde{\beta} + \tilde{\psi}) - \dot{\psi}_k x_e y_e \\ &\leq -k_x x_e^2 + 2U_{\max}(|y_e| + \Delta) \\ &= -k_x x_e^2 - k_x y_e^2 + 2U_{\max}(|y_e| + \Delta) + k_x y_e^2 \\ &= -k_x V_1 + 2U_{\max}(|y_e| + \Delta) + k_x y_e^2 \end{aligned} \quad (22)$$

where U_{\max} is the maximum of U , consider the sets $\Omega_s = \{(x_e, y_e) | x_e^2 + y_e^2 \leq \sigma_s\}$, where σ_s is a positive constant. (18) can be expressed by $\dot{V}_1 = -k_x V_1 + \Delta_e$, and $\Delta_e = 2U_{\max}(|y_e| + \Delta) + k_x y_e^2$.

4 Heading Control

4.1 Finite-Time Controller Design

The 4-DOF model of the sailboat is simplified to:

$$\begin{aligned} \dot{\psi} &= r \cos(\phi) \\ m_r \dot{r} &= M_{S_r} + F_r \delta_r - M_{K_r} - (X_{\dot{u}} - Y_{\dot{v}})uv - M_{D_r} - d|r|r \cos(\phi) + d w_r \end{aligned} \quad (23)$$

Simplification of rudder lift coefficient in this paper refer to [16].

The tracking error is defined as:

$$z_1 = \psi - \psi_d \quad (24)$$

Choosing the following appropriate virtual control laws:

$$\alpha_r = \frac{1}{\cos(\phi)} (-k_1 z_1 + \dot{\psi}_d - \beta_1 \text{sig}^\gamma(z_1)) \quad (25)$$

where k_0 is tuning parameter.

To avoid the ‘‘explosion of complexity’’, we replace $\dot{\theta}$ with $\dot{\alpha}_r$, and the finite-time filter is devised as

$$\begin{cases} \dot{\theta} = l \\ l = -\zeta_1 |\theta - \alpha_r|^{\frac{1}{2}} \text{sign}(\theta - \alpha_r) + \sigma_1 \\ \dot{\sigma}_1 = -\zeta_2 \text{sign}(\sigma_1 - l) \end{cases} \quad (26)$$

Lemma 3: ([26]) In the absence of input noise ($a_r = a_{r0}$), the filter is stable in finite time by choosing appropriate parameters ζ_1 and ζ_2 , and meet:

$$\sigma_1 = \alpha_{r0}, l = \dot{\alpha}_{r0} \quad (27)$$

Lemma 4: ([26]) Considering that the input noise satisfies $|\alpha_r - \alpha_{r0}| \leq \kappa$, the following inequality can be realized in finite time:

$$\begin{aligned} |\sigma_1 - \alpha_{r0}| &\leq \varpi_1 \kappa \\ |l - \dot{\alpha}_{r0}| &\leq \varpi_2 \kappa^{\frac{1}{2}} \end{aligned} \quad (28)$$

where ϖ_1, ϖ_2 are positive constants.

Define tracking error of α_r :

$$y_r = \theta - \alpha_r \quad (29)$$

Define error variable z_2 as follows

$$z_2 = r - \theta \quad (30)$$

The finite-time disturbance observer is devised as follows:

$$\begin{aligned}
m_r \dot{\hat{r}} &= A_1 + M_{Sr} + M_{Rr} - M_{Kr} - (X_{\dot{u}} - Y_{\dot{v}})uv - M_{Dr} - d|r|r \cos(\phi) \\
A_1 &= -\lambda_5 L_d^{1/2} \text{sig}^{1/2}(m_r \hat{r} - m_r r) + \hat{d}_{wr} \\
\dot{\hat{d}}_{wr} &= -\lambda_6 L_d \text{sgn}(\hat{d}_{wr} - A_1)
\end{aligned} \tag{31}$$

where λ_5, λ_6, L are positive constants.

Define error:

$$m_r \tilde{r} = m_r \hat{r} - m_r r \tag{32}$$

$$\tilde{d}_{wr} = \hat{d}_{wr} - d_{wr} \tag{33}$$

Derivation of the above error gives:

$$\begin{aligned}
m_r \dot{\tilde{r}} &= -\lambda_5 L_d^{1/2} \text{sig}^{1/2}(m_r \hat{r} - m_r r) + \hat{d}_{wr} + M_{Sr} + M_{Rr} - M_{Kr} \\
&\quad - (X_{\dot{u}} - Y_{\dot{v}})uv - M_{Dr} - d|r|r \cos(\phi) - m_r \dot{r} \\
&= -\lambda_5 L_d^{1/2} \text{sig}^{1/2}(m_r \tilde{r}) + \tilde{d}_{wr}
\end{aligned} \tag{34}$$

$$\dot{\tilde{d}}_{wr} = -\lambda_6 L_d \text{sign}(\hat{d}_{wr} - A_1) - d_{wr} \tag{35}$$

According to the lemma 2, the error of disturbance observation converges to zero in a finite time.

The control law is chosen as

$$\begin{aligned}
\alpha_M &= -M_{Sr} + M_{Kr} + (X_{\dot{u}} - Y_{\dot{v}})uv + M_{Dr} + d|r|r \cos(\phi) \\
&\quad + (-k_2 z_2 - k_3 \text{sig}^\gamma(z_2) + \dot{\theta})m_r - \hat{d}_{wr}
\end{aligned} \tag{36}$$

$$\delta'_r = \arcsin\left(\frac{2\alpha_M}{-1.2\rho A_R v_{dr}^2 |x_r|}\right) \tag{37}$$

Considering the rotation limit of the actuator rudder angle, limit the rudder angle:

$$\delta_r = \begin{cases} \delta'_r, & |\delta'_r| < \frac{\pi}{6} \\ \frac{\pi}{6} \text{sign}(\delta'_r), & |\delta'_r| \geq \frac{\pi}{6} \end{cases} \tag{38}$$

4.2 Stability Analysis

Select the following Lyapunov function:

$$V = \frac{1}{2}z_1^2 + \frac{1}{2}z_2^2 \tag{39}$$

Taking the derivation of the Lyapunov function, we get:

$$\dot{V} = z_1(\dot{\psi} - \dot{\psi}_d) + z_2(\dot{z}_2 - \dot{\theta})$$

$$\begin{aligned}
&= z_1[(z_2 + y_r + \alpha) \cos(\phi) - \dot{\psi}_d] + z_2(\dot{z}_2 - \dot{\theta}) \\
&= z_1 z_2 \cos(\phi) + z_1 y_r \cos(\phi) - k_1 z_1^2 - \beta_1 (z_1^2)^{\frac{\gamma+1}{2}} - k_2 z_2^2 - k_3 (z_1^2)^{\frac{\gamma+1}{2}} \quad (40)
\end{aligned}$$

It is known that the heel angle of the sailboat is bounded and will not exceed plus or minus $\frac{\pi}{2}$, so $0 < \cos(\phi) \leq 1$, the formula (36) can be simplified to:

$$\dot{V} \leq z_1 z_2 + z_1 y_r - k_1 z_1^2 - \beta_1 (z_1^2)^{\frac{\gamma+1}{2}} - k_2 z_2^2 - k_3 (z_1^2)^{\frac{\gamma+1}{2}} \quad (41)$$

According to Young's inequality

$$z_1 z_2 \leq \frac{1}{2} z_1^2 + \frac{1}{2} z_2^2 \quad (42)$$

$$z_1 y_r \leq \frac{1}{2} z_1^2 + \frac{1}{2} y_r^2 \quad (43)$$

By Lemma 3 and Lemma 4, y_r is a bounded value, so it has $|y_r| \leq d_1$. We have

$$\begin{aligned}
\dot{V}_1 &\leq \frac{1}{2} z_1^2 + \frac{1}{2} z_2^2 + \frac{1}{2} z_1^2 + \frac{1}{2} y_r^2 - k_1 z_1^2 - \beta_1 (z_1^2)^{\frac{\gamma+1}{2}} - k_2 z_2^2 - k_3 (z_1^2)^{\frac{\gamma+1}{2}} \\
&\leq -(k_1 - 1) z_1^2 - \beta_1 (z_1^2)^{\frac{\gamma+1}{2}} - (k_2 - \frac{1}{2}) z_2^2 - k_3 (z_1^2)^{\frac{\gamma+1}{2}} + \frac{1}{2} d_1^2 \quad (44)
\end{aligned}$$

From formula (40), the following inequality can be obtained:

$$\dot{V} \leq -aV - bV^{\frac{\gamma+1}{2}} + c \quad (45)$$

where $a = \min\{k_1 - 1, k_2 - \frac{1}{2}\}$, $b = \min\{\beta_1 2^{\frac{\gamma+1}{2}}, k_3 2^{\frac{\gamma+1}{2}}\}$, $c = \frac{1}{2} d_1^2$, according to the lemma 1, it can be known that the heading tracking system is stable in a limited time.

As shown in Fig. 3, DFLOS-AFC scheme and manual experience controls sail are combined for path following of sailboat.

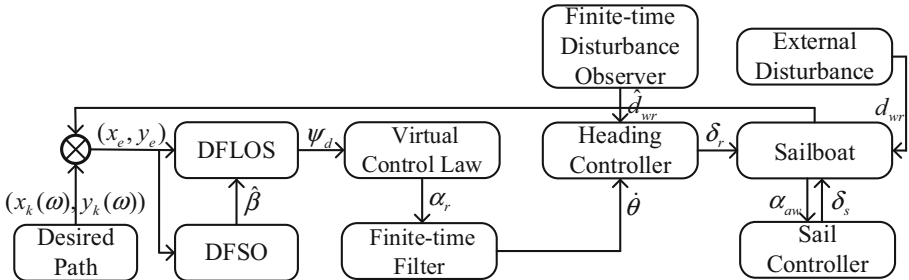


Fig. 3. Framework of sailboat control

5 Simulation Studies

To verify the feasibility of DFLOS-FC scheme, simulation study is conducted with 12 m class sailboat in [10]. The unknown external disturbances are assumed as follows

$$\begin{cases} d_{wu} = 500[0.2 \cos(0.1t) + 0.4 \sin(0.5t + \frac{\pi}{6}) + 0.8 \sin(t + \frac{\pi}{3})] \\ d_{wv} = 600[0.2 \sin(0.1t) + 0.4 \cos(0.5t + \frac{\pi}{6}) + 0.8 \sin(t + \frac{\pi}{3})] \\ d_{wp} = 100[0.2 \sin(0.1t) + 0.8 \sin(0.5t + \frac{\pi}{6}) + 0.4 \cos(t + \frac{\pi}{3})] \\ d_{wr} = 200[0.2 \sin(0.1t) + 0.4 \sin(0.5t + \frac{\pi}{6}) + 0.8 \sin(t + \frac{\pi}{3})] \end{cases} \quad (46)$$

The wind speed and the wind angle are set to 5m/s and $\psi_{tw} = 0^\circ$ respectively, and the parametric reference path is devised as

$$\begin{cases} x_k(\omega) = 70 \sin(0.01\omega) + 0.7\omega \\ y_k(\omega) = 0.7\omega \end{cases} \quad (47)$$

The design parameters of the DFLOS-FC scheme are chosen as follows: $k_x = 0.1$, $\lambda_1 = 4$, $\lambda_2 = 40$, $\lambda_3 = 4$, $\lambda_4 = 40$, $\vartheta_1 = 0.05$, $\vartheta_2 = 0.05$, $\Delta = 30$, $k_1 = 0.9$,

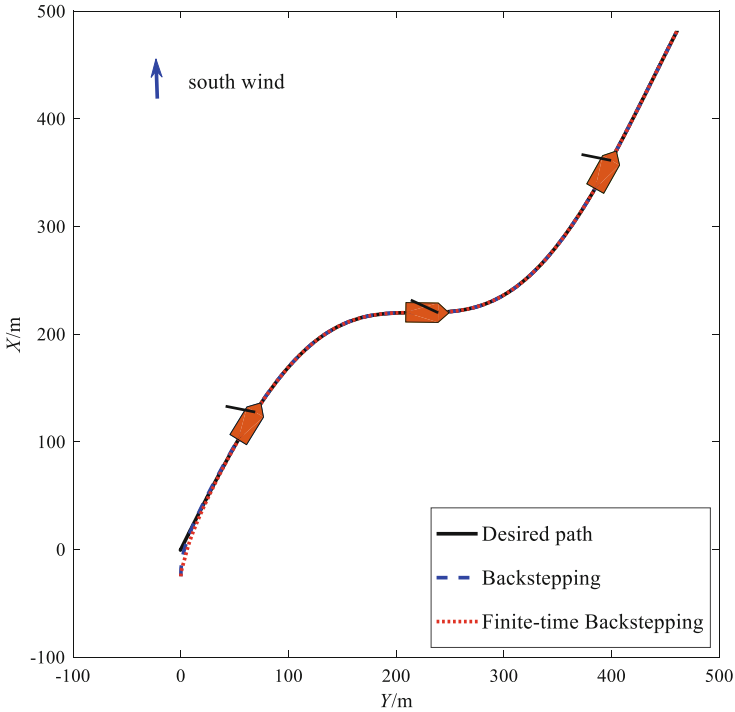


Fig. 4. Path following performance for sailboat

$\beta_1 = 0.01$, $\gamma = 0.6$, $\zeta_1 = 0.09$, $\zeta_2 = 0.001$, $\lambda_5 = 10$, $\lambda_6 = 10$, $L_d = 20$, $k_2 = 3$, $k_3 = 0.1$. Initial position of sailboat is $[-25 \text{ m}, 0 \text{ m}]$, and the remaining initial values are set to 0.

The simulation results of DFLOS-FC scheme are provided in Figs. 4, 5, 6, 7, 8, 9 and 10. In Fig. 4, the DFLOS-FC scheme achieves better performance in path following. As shown in Fig. 5, both along- and cross-track errors of DFLOS-FC can converge to zero in a shorter time. Compared with the traditional backstepping method, DFLOS-FC has better convergence effect and does not produce jitter. In Fig. 6, The convergence speed of DFLOS-FC is faster than that of traditional backstepping method. The estimated sideslip angle is shown in Fig. 7. Figure 8 shows that the designed finite time disturbance observer can accurately observe external disturbance. The variation of rudder angle and sail angle with time is shown in Fig. 9. As shown in Fig. 10, the maximum roll angle does not exceed 30° , which is in line with the sailing practice.

The presented results clearly indicate that the proposed DFLOS-FC schemes work well for path following of sailboat.

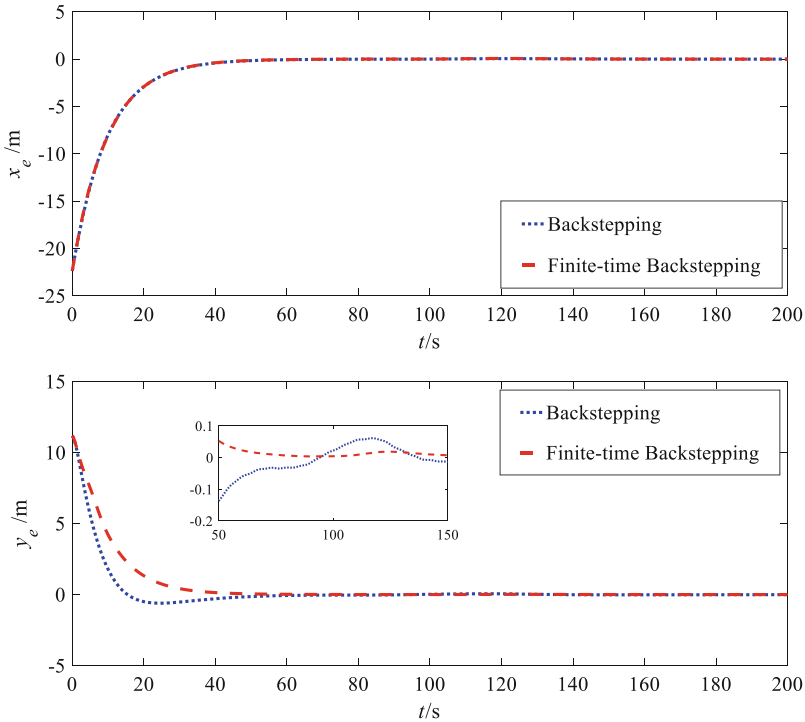


Fig. 5. Path tracking error (x_e, y_e)

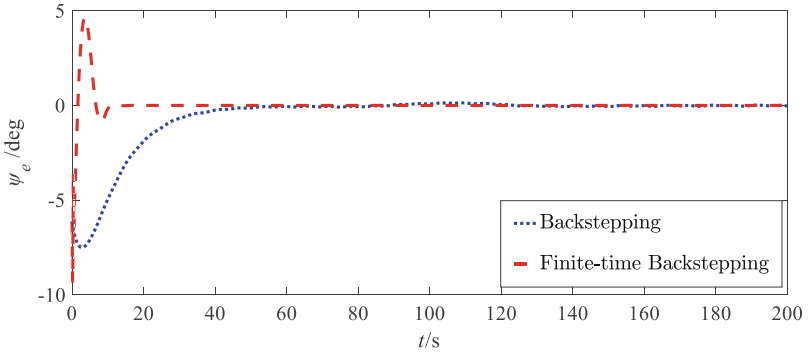


Fig. 6. Heading tracking error (ψ_e)

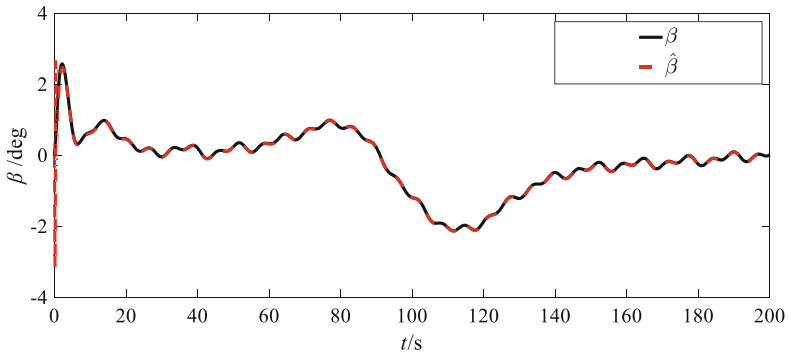


Fig. 7. Sideslip angle observation

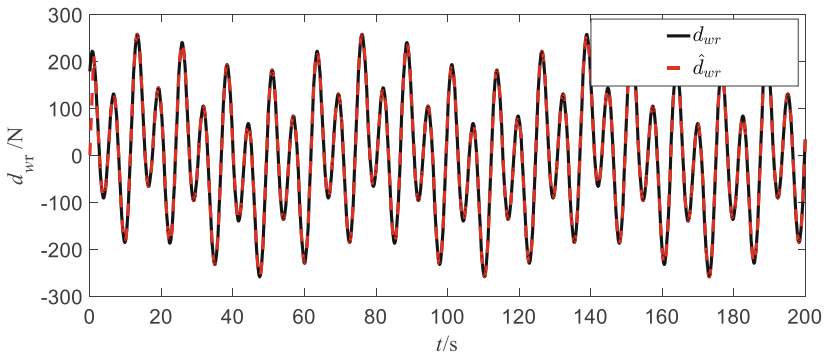


Fig. 8. External disturbance observation

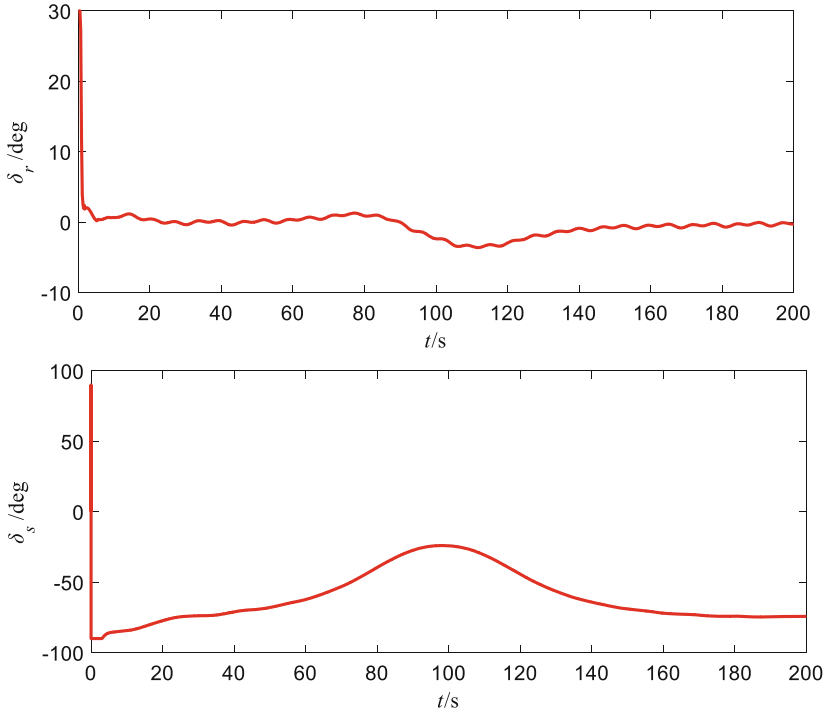


Fig. 9. Control inputs δ_r and δ_s

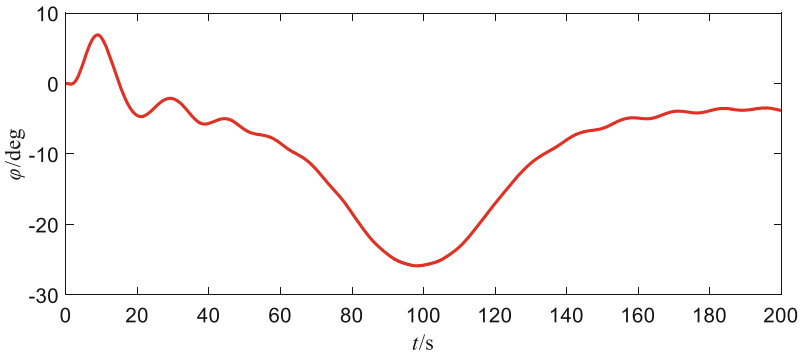


Fig. 10. Variation of sailboat roll angle

6 Conclusion

In this paper, considering the problem of accurate path following of sailboat under no upwind sailing, a LOS guidance framework based on double finite-time sideslip angle observers is proposed. The time-varying sideslip angle is accurately estimated by the DFSO, and the observation error can converge to the origin at short notice. The simulation results show that the designed DFLOS-FC has higher path tracking accuracy and

smaller horizontal and vertical tracking errors. In the heading control system, the external disturbance is estimated by finite-time disturbance observer to reduce the computational complexity of the system. Eventually, Compared with the ordinary backstepping method, the designed DFLOS-FC converges faster and has a good convergence effect.

References

1. Manley, J.: Unmanned surface vehicles, 15 years of development. In: OCEANS 2008 Conference, Quebec City, Canada, pp. 1–3 (2008)
2. Wang, N., Zhang, Y.: Autonomous pilot of unmanned surface vehicles: Bridging path planning and tracking. *IEEE Trans. Veh. Technol.* **71**(3), 2358–2374 (2022)
3. Pettersen, K., Lefeber, A.: Way-point tracking control of ships. In: IEEE Conference on Decision and Control, Orlando, FL, USA, pp. 940–946. IEEE (2001)
4. Li, J., Lee, P., Jun, B., Lim, Y.: Point-to-point navigation of underactuated ships. *Automatica* **44**(12), 3201–3205 (2008)
5. Wan, L., Su, Y., Zhang, H.: An improved integral light-of-sight guidance law for path following of unmanned surface vehicles. *Ocean Eng.* **205**(3), 3–6 (2020)
6. Su, Y., Wan, L.: An improved adaptive integral line-of-sight guidance law for unmanned surface vehicles with uncertainties. *Appl. Ocean Res.* **108**(5), 3–7 (2020)
7. Liu, Z.: Improved ELOS based path following control for underactuated surface vessels with roll constraint. *Ocean Eng.* **245**(1), 2–8 (2022)
8. Wang, N., Gao, Y., Zhang, X.: Data-driven performance-prescribed reinforcement learning control of an unmanned surface vehicle. *IEEE Trans. Neural Netw. Learn. Syst.* **32**(12), 5456–5467 (2021)
9. Dos Santos, D., Goncalves, L.: A gain-scheduling control strategy and short-term path optimization with genetic algorithm for autonomous navigation of a sailboat robot. *Int. J. Adv. Rob. Syst.* **16**(1), 2–7 (2019)
10. Viel, C., Vautier, U., Wan, J., Jaulin, L.: Position keeping control of an autonomous sailboat. *IFAC-PapersOnLine* **51**(29), 14–19 (2018)
11. Wille, K., Hassani, V., Sprenger, F.: Modeling and course control of sailboats. *IFAC PapersOnLine* **49**(23), 532–539 (2016)
12. Xiao, L., Jouffroy, J.: Modeling and nonlinear heading control of sailing yachts. *IEEE J. Oceanic Eng.* **39**(2), 256–268 (2014)
13. Wang, N., Qian, C., Sun, J.C.: Adaptive robust finite-time trajectory tracking control of fully actuated marine surface vehicles. *IEEE Trans. Control Syst. Technol.* **24**(4), 1454–1462 (2016)
14. Wang, N., Karimi, H.R., Li, H.: Accurate trajectory tracking of disturbed surface vehicles: a finite-time control approach. *IEEE/ASME Trans. Mechatron.* **24**(3), 1064–1074 (2019)
15. Hou, Q., Ma, L.: Composite finite-time straight-line path-following control of an underactuated surface vessel. *ScienceDirect* **357**(16), 11496–11517 (2020)
16. Wang, N., He, H.: Extreme learning-based monocular visual servo of an unmanned surface vessel. *IEEE Trans. Industr. Inf.* **17**(8), 5152–5163 (2021)
17. Deng, Y., Zhang, X., Zhang, Q., Hu, Y.: Event-triggered composite adaptive fuzzy control of sailboat with heeling constraint. *Ocean Eng.* **211**(1), 2–5 (2020)
18. Wang, N., Er, M.J.: Self-Constructing adaptive robust fuzzy neural tracking control of surface vehicles with uncertainties and unknown disturbances. *IEEE Trans. Control Syst. Technol.* **23**(3), 991–1002 (2015)
19. Wang, N., Meng, J.E.: Direct adaptive fuzzy tracking control of marine vehicles with fully unknown parametric dynamics and uncertainties. *IEEE Trans. Control Syst. Technol.* **24**(5), 1845–2185 (2016)

20. Wang, N., Er, M.: Adaptive robust online constructive fuzzy control of a complex surface vehicle system. *IEEE Trans. Cybern.* **46**(7), 1511–1523 (2016)
21. Cui, R., Zhang, X., Cui, D.: Adaptive sliding-mode attitude control for autonomous underwater vehicles with input nonlinearities. *Ocean Eng.* **123**(1), 45–54 (2016)
22. Wang, N., Su, S.: Finite-time unknown observer based interactive trajectory tracking control of asymmetric underactuated surface vehicles. *IEEE Trans. Control Syst. Technol.* **29**(2), 794–803 (2021)
23. Yu, J., Shi, P., Zhao, L.: Finite-time command filtered backstepping control for a class of nonlinear systems. *Automatica* **92**, 173–180 (2018)
24. Shtessel, Y., Shkolnikov, I., Levant, A.: Smooth second-order sliding modes: missile guidance application. *Automatica* **43**(8), 1470–1476 (2007)
25. Basin, M., Yu, P., Shtessel, Y.: Finite- and fixed-time differentiators utilising HOSM techniques. *IET Control Theory Appl.* **11**(8), 1144–1152 (2016)
26. Zhao, L., Yu, J., Lin, C., Ma, Y.: Adaptive neural consensus tracking for nonlinear multiagent systems using finite-time command filtered backstepping. *IEEE Trans. Syst. Man Cybern. Syst.* **48**(11), 2003–2012 (2018)